

ARAŞTIRMA MAKALESİ / RESEARCH ARTICLE

ADSORPTION OF Ni(II) IONS FROM AQUEOUS SOLUTIONS ONTO MAGNETIC-POLY(DIVINYLBENZENE-CO-VINYLIMIDAZOLE) MICROBEADS: PHYSICOCHEMICAL STUDIES

Ali KARA¹, Emel DEMİRBEL¹

ABSTRACT

A modified suspension polymerization was used for the preparation of the mesoporous magnetic-poly(divinylbenzene-co-vinylimidazole) (m-poly(DVB-VIM)) microbeads in size 53-212 μm of average diameter. The specific surface area and the DVB/VIM mol ratio of the microspheres were determined as $29.47 \text{ m}^2/\text{g}$ and 1:4 mol/mol with Fe_3O_4 , respectively. The physicochemical studies of adsorption of Ni(II) ions from aqueous solutions such as pH, initial concentration, amount of mesoporous m-poly(DVB-VIM) microbeads, contact time, and temperature onto the m-poly(DVB-VIM) microspheres were carried out. The maximum adsorption capacities of the m-poly(DVB-VIM) microspheres towards Ni(II) ions were determined as 13.51, 20.14, 21.00 and 23.62 mg/g at 277 K, 298 K, 318 K, and 338 K, respectively. The dynamic and equilibrium adsorption behaviours of the system were adequately described by the pseudo-second-order kinetic and the Langmuir isotherm models, respectively. Various thermodynamic parameters, such as the Gibbs' free energy change (ΔG°), the standard enthalpy change (ΔH°) and the standard entropy change (ΔS°) were also determined. Moreover, after use in the adsorption, the m-poly(DVB-VIM) microbeads with paramagnetic property was separated from the via the applied magnetic force. These results indicate that the material studied could be used as a purifier for the removal of Ni(II) ions from water and wastewater under magnetic field.

Keywords: Magnetic polymers; Adsorption isotherm; Adsorption kinetic; Adsorption thermodynamic; Ni(II) ions.

¹, Department of Chemistry, Uludag University, Görükle Campus, Nilüfer 16059, Bursa, Turkey.

Tel and Fax: (90) 224 2941733 e-mail: akara@uludag.edu.tr

e-mail: Emel Demirbel: emeldemirbel@uludag.edu.tr

MANYETİK-POLİ(DİVİNİL BENZEN-KO-VİNİLİMİDAZOL) MİKROKÜRELER ILE SULU ÇÖZELTİLERDEN Ni(II) İYONLARININ ADSORPSİYONU: FİZİKOKİMYASAL ÇALIŞMALARI

ÖZ

Ortalama çapı 53-212 μm olan mezogözenekli manyetik-poli(divinilbenzen-ko-vinilimidazol) (m-polí(DVB-VIM)) mikrokürelerinin hazırlanması için modifiye süspansiyon polimerizasyonu kullanıldı. Mikrokürelerin spesifik yüzey alanı $29.47 \text{ m}^2\text{g}^{-1}$ ve Fe_3O_4 ilavesiyle birlikte, DVB/VIM mol oranı 4:1 mol/mol olarak belirlendi. Fizikokimyasal çalışmalar m-polí(DVB-VIM) mikroküreleri üzerine pH, başlangıç konsantrasyonu, mikroküre miktarı, temas süresi ve sıcaklık gibi parametrelerle incelendi. m-polí(DVB-VIM) mikrokürelerinin Ni(II) iyonlarına karşı maksimum adsorpsiyon kapasitesi 277 K, 298 K, 318 K ve 338 K'de sırasıyla 13.51, 20.14, 21.00 ve 23.62 mg.g^{-1} olarak belirlendi. Sistemin dinamik ve denge adsorpsiyon davranışları sırasıyla yalancı ikinci derece model ve Langmuir izoterm modeliyle açıklandı. Gibbs serbest enerji değişimi (ΔG°), standart entalpi değişimi (ΔH°) ve standart entropi değişimi (ΔS°) gibi termodinamik parametreler belirlendi. Ayrıca adsorpsiyonda kullanımdan sonra, paramanyetik özellikli m-polí(DVB-VIM) mikroküreleri uygulanan manyetik kuvvet yardımıyla ayrıldı. Bu sonuçlar, çalışılan malzemenin manyetik alan altında su ve atık sulardan Ni(II) iyonlarının uzaklaştırılması için kullanılabilir olduğunu gösterdi.

Anahtar Kelimeler: Manyetik polimerler; Adsorpsiyon izotermi; Adsorpsiyon kinetiği; Adsorpsiyon termodinamigi; Ni (II) iyonları.

Notation

- C_e concentration of Ni(II) ions at equilibrium (mg L^{-1})
- C_0 initial concentration of Ni(II) ions in solution (mg L^{-1})
- E_a activation energy of adsorption (kJ mol^{-1})
- E_{fe} free energy of adsorption (kJ mol^{-1})
- ΔG° Gibbs free energy of adsorption (J mol^{-1})
- ΔH° isosteric enthalpy of adsorption (J mol^{-1})
- ΔS° entropy change of the adsorption process ($\text{J mol}^{-1} \text{ K}^{-1}$)
- q_e the amount of Ni(II) ions adsorbed on the adsorbent at equilibrium (mg g^{-1})
- q_t the amount of Ni(II) ions adsorbed on the adsorbent at any time (mg g^{-1})
- q_m the maximum amount of Ni(II) ions adsorbed per unit mass adsorbent (mg g^{-1})
- Q_L the maximum amount of Ni(II) ions adsorbed per unit mass adsorbent (mg g^{-1})
- K_L the Langmuir constant related to the affinity of binding sites (mL mg^{-1})
- n the heterogeneity factor
- K_F the Freundlich constant
- Q_{D-R} the maximum amount of Ni(II) ions adsorbed per unit mass adsorbent (mg g^{-1})
- K_{D-R} the Dubinin-Radushkevich constant ($\text{mol}^2 \text{ J}^{-2}$)
- ε the Polanyi potential (J mol^{-1})
- R_L the dimensionless separation factor
- k_1 the rate constant of pseudo first-order adsorption (min^{-1})
- k_2 the rate constant of pseudo second-order adsorption ($(\text{g/mg}) \text{ min}^{-1}$)
- k_R the rate constant for the modified Ritchie's-second-order model (min^{-1})
- k_i the intraparticle diffusion rate constant ($\text{mg/g min}^{0.5}$)
- R^2 linear regression coefficient
- t time (min)
- T temperature (K)

1. INTRODUCTION

Nickel, comparatively a rare metal in nature, is a toxic heavy metal ion present in water and wastewater. The main source of nickel pollution in the water and wastewater derives from industrial production processes such as stainless steel, galvanization, electroplating, batteries manufacturing, the manufacturing of magnetic tape, jewelry and coinage, in welding rods, as a catalyst in oil hydrogenation and coal gasification, dental procedures, electric storage batteries, pigments and so on. The presence and accumulation of nickel in industrial effluents has a toxic or carcinogenic effect such as headache, dizziness, nausea and vomiting, chest pain, tightness of the chest, shortness of breath, rapid respiration, cyanosis, extreme weakness on human health. Thereby, it is of great importance to eliminate nickel ions from waste and wastewaters (Patil and Shrivastava, 2010, Strkalj et al, 2010, Akgol et al, 2006).

The high consumption of nickel-containing products inevitably leads to environmental pollution by nickel and its derivatives at all stages of production, utilization, and disposal. The physicochemical methods such as precipitation/neutralization, ultrafiltration, reverse osmosis, electrodeposition, solvent extraction, foamb flotation, cementation, complexation, filtration, evaporation, ion exchange, and adsorption have been used to remove Ni(II) ions from wastewater. Adsorption is one of the most versatile methods for the removal of Ni(II) ion contamination from aqueous systems. Some of the adsorption processes have managed to complete in a short time. In recent years, the adsorption of Ni(II) ions by magnetic polymers has attracted significant attention. Magnetic polymers have several potential advantages over conventional approaches. In this technique, Ni(II) ions to be separated can be directly transported by convection to the binding sites on the surface of the adsorbent, higher throughput and faster processing times onto the magnetic particles can be achieved. (Monier et al, 2010, Ozay et al, 2009, Hua et al, 2011, Mahdavian and Mirrahim, 2010, Wang et al, 2010)

The physicochemical studies of adsorption for Ni(II) ions presented herein is a part of the

investigations conducted to evaluate the effectiveness of magnetic polymers. This study provides insight into Ni(II) ions adsorption from aqueous solutions in terms of equilibrium and kinetics. It also provides important information that could be used in the design and optimization of Ni(II) ions adsorption operations. Furthermore, the results of this study could be helpful in the prediction of the Ni(II) ions rate of transport. The effects of various system parameters such as pH, initial concentration, contact time, temperature, amount and repeated use of m-poly(DVB-VIM) microbeads were systematically studied and the results obtained are discussed.

2. EXPERIMENTAL

2.1 Materials

Divinylbenzene (DVB, 98%) obtained from Merck (Darmstadt, Germany) was vacuum-distilled after being washed with an aqueous 10% NaOH solution. 1-vinylimidazole (VIM, Aldrich, Steinheim, Germany) was distilled under vacuum (74–76°C, 10 mmHg). 2,2'-Azobisisobutyronitrile (AIBN) was obtained by Merck (Darmstadt, Germany). Poly(vinyl alcohol) (PVA; Mw: 72000, 98% hydrolyzed) was supplied from Merck (Darmstadt, Germany). Magnetite nanopowder (Fe_3O_4 ; diameter 20–30 nm) was obtained from Aldrich (USA). Nickel nitrate hexahydrate was supplied by Fluka (Hannover, Germany). All other reagents, unless specified, were of analytical grade and were used without further purification. Laboratory glassware was kept overnight in a 5% nitric acid solution. Before use the glassware was rinsed with deionized water and dried in a dust-free environment. All water used in the adsorption experiments was purified using a Barnstead (Dubuque, IA, USA) ROpure LP® reverse osmosis unit with a high flow cellulose acetate membrane (Barnstead D2731) followed by a Barnstead D3804 NANOpure® organic/colloid removal and ion exchange packed-bed system.

2.2 Synthesis of m-poly(DVB-VIM) Microbeads

DVB and VIM were copolymerized in suspension by using AIBN and poly(vinyl alcohol)

as the initiator and stabilizer, respectively. Toluene was included in the polymerization recipe as the diluent (as a pore former). A typical preparation procedure is described here. A continuous medium was prepared by dissolving poly(vinyl alcohol) (200 mg) in the purified water (50 mL). For the preparation of the dispersion phase, DVB (2.9 ml; 20 mmol) magnetite Fe_3O_4 nanopowder (0.5 g) and toluene (10 mL) were stirred for 10 min at room temperature. Then, VIM (7.3 ml; 80 mmol) and AIBN (100 mg) were dissolved in the homogeneous organic phase. The organic phase was dispersed in the aqueous medium by stirring the mixture magnetically (500 rpm) in a sealed-cylindrical pyrex polymerization reactor. The reactor content was heated to polymerization temperature (i.e., 65 °C) within 4 h and the polymerization was conducted for 2 h with a 600 rpm stirring rate at 80 °C. The final microbeads were extensively washed with ethanol and water to remove any unreacted monomer or diluent and then dried at 50 °C in a vacuum oven. The microbeads then were sieved to different sizes. An inspection with a microscope showed that almost all the microbeads were perfectly spherical form of 53–212 µm in diameter.

2.3 Characterization Experiments of m-poly(DVB-VIM) Microbeads

The porosity of the microbeads was measured by a N_2 gas adsorption/desorption isotherm technique (Quantachrome Corporation, Poremaster 60, USA). The specific surface area of beads in a dry state was determined by a multipoint Brunauer-Emmett-Teller (BET) apparatus (Quantachrome Corporation, Autosorb-6, USA). 0.0806 g of bead was placed in the sample holder of the BET and degassed by passing through N_2 gas onto the beads at 60 °C for 315 min. The adsorption of the N_2 gas onto the microbeads was performed at 77.40 K while its desorption was performed at room temperature. Experimental values obtained from the desorption step were used to calculate the specific surface area of the beads. Pore volumes and average pore diameter for the beads were determined by the BJH (Barrett, Joyner, Halenda) model. The average size and size distribution of the beads were determined by screen analysis performed using standard sieves (Model AS200,

Retsch Gmb & Co., KG, Haan, Germany). The water uptake ratios for the beads were determined using distilled water. The water uptake experiments were conducted as follows: Dry beads were carefully weighed out (+0.0001 g) before being soaked into 50 mL vials containing distilled water. The vials were then placed in an isothermal water bath at 25 °C for 2 h after which the wet bead samples were taken out of the vials, wiped out with a filter paper, and weighed out. The water content of the beads was calculated by using the following expression:

$$\text{Water uptake (\%)} = \left[\frac{W_s - W_o}{W_o} \right] \times 100 \quad (1)$$

where W_o and W_s are the weights of beads before and after water uptake, respectively.

After the bead samples were dried at 25 °C for 7 days, tiny fragments of the bead samples were mounted on SEM sample holders on which they were sputter coated for 2 min. The samples were then consecutively mounted in a scanning electron microscope (Carl Zeiss EVO 40, UK) to visualize the surface structures of each bead sample at desired magnification levels. In order to evaluate the degree of VIM incorporation, the synthesized m-poly(DVB-VIM) microbeads were subjected to elemental analysis using a Leco Elemental Analyzer (Model CHNS-932, USA). The magnetization curve of the bead sample was measured by a vibrating sample magnetometer (VSM, Princeton Applied Research, Model 150A, USA). The presence of magnetite nano-powders in the bead samples was investigated with an electron spin resonance (ESR) spectrophotometer (EL 9, Varian, USA).

2.4 Adsorption Experiments

Batch adsorption experiments were performed using 0.050 g of the m-poly(DVB-VIM) microbeads in 100 mL-Erlenmeyer flasks with 50 mL of aqueous metal ion solutions. The sample was shaken at 300 rpm in a shaking water bath (Clifton, England). After the desired contact time, the suspension was filtered. The filtrate was analyzed for metal ions by using ICP-OES (Perkin Elmer, Optima 2100 DV). The amount of Ni(II) ions adsorbed onto the

microbeads was calculated from the difference between the initial and the final concentrations.

2.5 Desorption and Repeated Use Experiments

Ni(II) ions adsorbed onto the m-poly(DVB-VIM) microbeads were desorbed in 0.1 M HNO₃ in a shaking water bath (Clifton, England) at 300 rpm for 2 h at room temperature. The final Ni(II) ions concentration in the desorption medium was determined using ICP-OES (Perkin Elmer, Optima 2100 DV). The desorption ratio was calculated from the amount of Ni(II) ions adsorbed on the m-poly(DVB-VIM) microbeads and the final Ni(II) ions concentration in the desorption medium by using the following expression.

$$\text{Desorption ratio} = \frac{\text{Amount of Ni(II)ions desorbed to the desorption medium}}{\text{Amount of Ni(II)ions adsorbed on the microbeads}} \times 100 \quad (2)$$

In order to determine the reusability of the mesoporous magnetic microbeads, consecutive adsorption-desorption cycles were repeated 10 times using the same magnetic microbeads.

3. RESULTS AND DISCUSSION

3.1 Characterization of m-poly(DVB-VIM) Microbeads

The suspension polymerization procedure provided here cross-linked the m-poly(DVB-VIM) microbeads in the spherical form of 53–212 µm in diameter. The N₂ adsorption/desorption isotherms for the m-poly(DVB-VIM) and the calculated pore size distributions are plotted (not shown). The BET surface area ($S_{BET} = 29.47 \text{ m}^2 \text{ g}^{-1}$), pore volume ($V_p = 0.073 \text{ cm}^3 \text{ g}^{-1}$), and BJH pore size ($P_{BJH} = 3.761 \text{ nm}$) were found (not shown). The sample gave a type IV Standard isotherm with a deep inflection between relative pressure P/P_o = 0.4 and 0.9, characteristic of capillary condensation, indicating the uniformity of the mesopore-size distribution (Duan et al, 2008, Souza et al, 2009, Fu et al, 2007). This indicated that the magnetic beads contained mainly mesopores. The equilibrium swelling ratio for the m-poly(DVB-VIM) microbeads is 44%. It should be also noted that due to their highly cross-linked structure, these

microbeads are strong enough to be suitable for column applications. The surface morphology and bulk structures of the m-poly(DVB-VIM) microbeads were visualized by SEM, as presented in Figure 1. All the beads have a spherical form and rough surface. In the SEM photograph of the bulk structure, a large quantity of well-distributed pores could be observed and they have a netlike structure. In order to facilitate diffusion of Ni(II) ions, the m-poly(DVB-VIM) microbeads prepared in this study had large pores.

The m-poly(DVB-VIM) microbeads were synthesized by copolymerizing DVB with VIM at a 1:4 molar ratio with Fe₃O₄ in the presence of the initiator AIBN. To evaluate the degree of VIM incorporation into the m-poly(DVB-VIM) microbeads, elemental analysis (C: 80.74%; H: 7.48%; N: 4.23%) of the synthesized m-poly(DVB-VIM) microbeads was performed. The incorporation of the VIM was found to be 3.021 mmol/g polymer from the nitrogen stoichiometry.

Magnetic characteristics of magnetic materials are usually related to the content of the magnetic component. It follows that Fe₃O₄ content is very important to the magnetic responsiveness of magnetic materials. In general, a higher Fe₃O₄ content shows a stronger magnetic responsiveness (Tseng et al, 2007). For this reason, the average Fe₃O₄ content of the m-poly(DVB-VIM) microbeads was determined by density analysis. The hydrated density of the m-poly(DVB-VIM) microbeads measured at 25 °C was 1.41 g/mL. By the same procedure, the density of Fe₃O₄ particles was found to be 4.94 g/mL at 25 °C. The density of non-magnetic poly(DVB-VIM) microbeads measured at 25 °C was 1.01 g/mL. The magnetic particles volume fraction in the m-poly(DVB-VIM) microbeads can be calculated from the following equation derived from the mass balance:

$$\phi = (\rho_c - \rho_m) / (\rho_c - \rho_a) \quad (3)$$

Where, ρ_A , ρ_c and ρ_M are the densities of non-magnetic poly(DVB-VIM) microbeads, Fe₃O₄ nanopowder, and the m-poly(DVB-VIM) microbeads, respectively. Thus, with the density data mentioned above, the m-poly(DVB-VIM)

microbeads gel volume fraction in the magnetic beads was estimated to be 89.2%. Therefore, the average Fe_3O_4 content of the resulting m-poly(DVB-VIM) microbeads was 10.2%. The presence of magnetite nanopowder in the polymer structure was also confirmed by the ESR (not shown). A peak of magnetite was detected in the ESR spectrum. It should be noted that the non-magnetic beads cannot be magnetized under this condition. It reflects response ability of magnetic materials to the change of external magnetic field firstly and it characterizes the ability of magnetic materials to keep magnetic field strength when the external magnetic field is removed. In order to show the magnetic stability, the m-poly(DVB-VIM) microbeads were kept in distilled water and ambient air for 3 months, and the same ESR spectrum was obtained. With the goal of testing the mechanical stability of the m-poly(DVB-VIM) microbeads, a bead sample was treated in a ball mill for 12 h. SEM photographs showed that a zero percentage of the sample was broken. The g factor can be considered as the quantity characteristic of the molecules in which the unpaired electrons are located, and it is calculated from Equation (4). The measurement of the g factor for an unknown signal can be a valuable aid in the identification of a signal. In the literature, the g factor for Fe(III) is determined between 1.4 – 3.1 for low spin and 2.0 – 9.7 for high spin complexes (Senel et al, 2008). The g factor was found to be 2.44 for the m-poly(DVB-VIM) microbeads structure.

$$g = \frac{h \cdot \vartheta}{\beta \cdot H_r} \quad (4)$$

Here, h is the Planck constant (6.626×10^{-27} erg s $^{-1}$); β is the universal constant (9.274×10^{-21} erg G $^{-1}$); ϑ is frequency (9.707×10^9 Hz), and H_r is the resonance of the magnetic field (G).

3.2 Effect of pH on Adsorption of Ni(II) ions

The adsorption of the metal ions onto an adsorbent varies generally with pH because pH causes changes to the radius of the hydrolyzed cation and the charge of the adsorbent surface. Therefore, in this study, the adsorption of Ni(II) ions onto the m-poly(DVB-VIM) microbeads was studied as a function of pH. The initial pH values of Ni(II) solutions were kept between 2.0

and 6.0. The relationship between initial pH and the amounts of Ni(II) ions adsorbed on the m-poly(DVB-VIM) microbeads for initial solution concentrations of 100 mg dm $^{-3}$ for at 298 K and a contact time of 60 min is illustrated in Figure 2. When initial pH values of Ni(II) solutions were increased from 2.0 to 6.0, the amounts of Ni(II) ions adsorbed per unit mass of adsorbent increased. For example, the amounts of Ni(II) ions adsorbed per unit mass of adsorbent increased from 2.08 to 16.35 mg g $^{-1}$ for Ni(II) ions when the pH value increased from 2.0 to 6.0. As seen in Figure 2, pH 6.0 is a value for the maximum adsorption of Ni(II) ions. The m-poly(DVB-VIM) microbeads exhibited a low affinity for Ni(II) ions in acidic conditions (pH=4.0), with a somewhat higher affinity at pH=6.0. The difference in binding behavior of Ni(II) ions can be explained by the different affinity of Ni(II) ions for the donor atoms (i.e., nitrogen) in the VIM (Kara et al, 2004).

3.3 Effect of Temperature on Adsorption of Ni(II) ions

The uptake of Ni(II) ions (mg g $^{-1}$) was increased from 11.02 to 21.93 mg g $^{-1}$ with the rise in temperature from 277 K to 338 K (Figure 3). Equilibrium time was found to be 60 min. indicating that the equilibrium time was independent of temperature. The above results also showed that the adsorption was endothermic in nature. The imidazole groups of the m-poly(DVB-VIM) microbeads are partially protonated at all temperatures but their deprotonation degree decreases at higher temperatures, resulting in a slight increase in the capacities of Ni(II) ions at high temperature. Where only adsorption of Ni(II) ions is involved, the temperature effect on retention time is relatively small. Empirical studies show that temperature has a small effect on adsorption (Tseng et al, 2007, Ozer et al, 2004, Bayramoglu et al, 2006, Bajpai and Johnson, 2007, Hanafiah et al, 2010, Taqvi et al, 2008).

3.4 Effect of Adsorbent Dosage on Adsorption of Ni(II) ions

The effect of adsorbent dosage on the adsorption of Ni(II) ions is shown in Figure 4. The percentage removal increases from 16.3% to 100.0% by increasing the adsorbent dosage from 50 to 1000 mg.

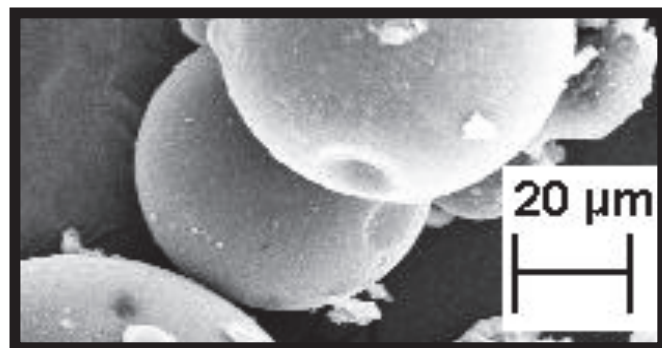


Figure 1. SEM photograph of the m-poly(DVB-VIM) microbeads.

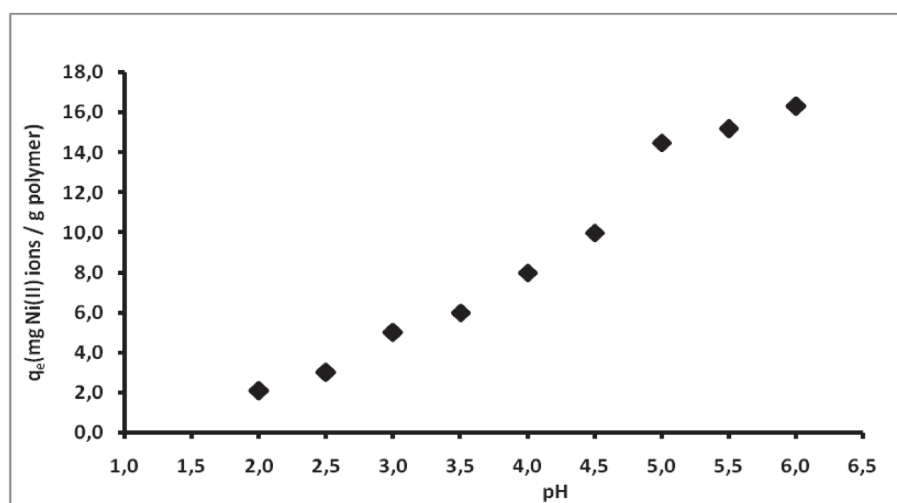


Figure 2. Effect of pH on adsorption of Ni(II) ions onto the m-poly(DVB-VIM) microbeads.

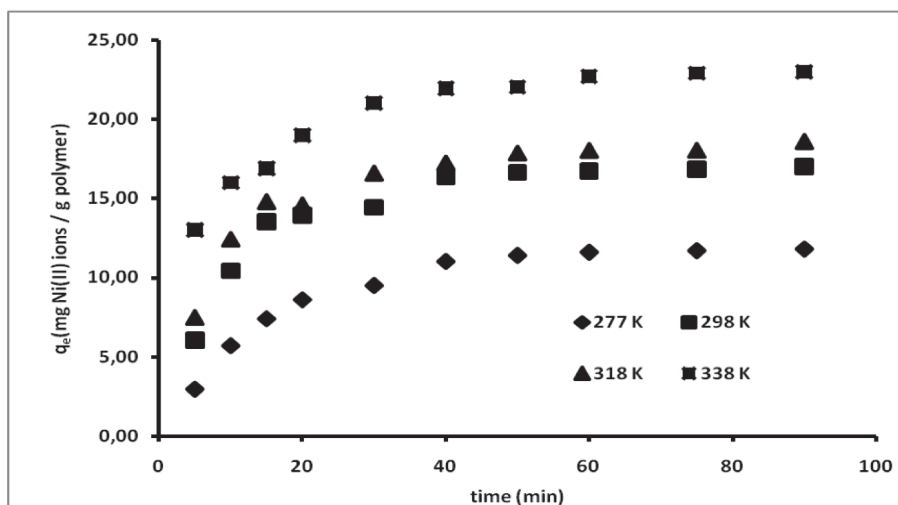


Figure 3. Effect of temperature on adsorption of Ni(II) ions onto the m-poly(DVB-VIM) microbeads.

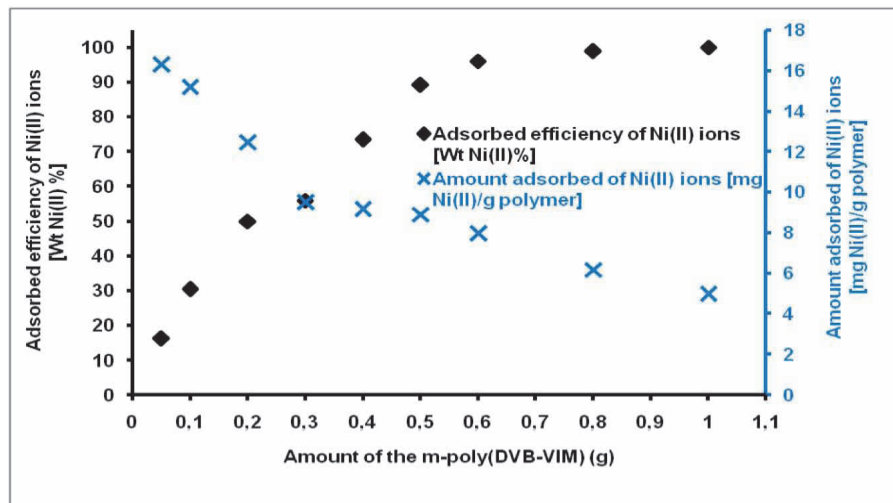


Figure 4. Effect of adsorbent dosage on adsorption of Ni(II) ions.

The adsorption capacity dropped from 16.3 to 5.01 mg/g by increasing the adsorbent dosage from 50 to 1000 mg. It is apparent from Figure 4 that by increasing the resin amount, the adsorption efficiency increases but adsorption density, the amount adsorbed per unit mass, decreases. It is readily understood that the number of available adsorption sites increases by increasing the adsorbent amount but the drop in adsorption capacity is basically due to the sites remaining unsaturated during the adsorption process (Olgun and Atar, 2011, Ghassabzadeh et al, 2010, Ngah and Fatinathan, 2010, Hanafiah et al, 2009).

3.5 Effect of Initial Concentration of Ni(II) ions on Adsorption of Ni(II) ions

Ten different concentrations for Ni(II) ions, i.e., concentrations of 25, 50, 75, 100, 150, 200, 250, 300, 350 and 400 mg·dm⁻³, were selected to investigate the effect of the initial concentration of Ni(II) ions onto the m-poly(DVB-VIM) microbeads. The amounts of Ni(II) ions adsorbed at equilibrium at 277, 298, 318, and 333 K, respectively, and pH 6.0 are graphed in Figure 5. As shown in Figure 5, with increasing initial concentration of Ni(II) ions from 25 to 400 mg dm⁻³, the amount of Ni(II) ions adsorbed by adsorbent increases from 3.60 to 14.92, from 4.11 to 21.16, from 4.85 to 22.59, and from 5.97 to 24.00 mg g⁻¹ of polymer at 277, 298, 318, and 333 K, respectively.

3.6 Adsorption Kinetics

Numerous adsorption processes have been investigated, particularly during the past 25 years. It has been known that adsorption process could be dependent on and controlled by different kinds of mechanisms such as diffusion control, mass transfer, chemical reactions and particle diffusion. The pseudo-first-order kinetic model, pseudo-second-order kinetic model, modified Ritchie's-second-order kinetic model, and intraparticle diffusion model were used for testing dynamic experimental data at the initial concentration, 100 mg/L, of Ni(II) ions and four temperatures (277, 298, 318 and 338 K) in pH 6.0.

The pseudo-first-order kinetic model of Lagergren is given as follows (Lagergren, 1898)

$$\log (q_e - q_t) = \log q_e - k_1 t / 2.303 \quad (5)$$

where q_e and q_t (mg/g) are the amounts of the Ni(II) ions adsorbed at equilibrium and at time (min), respectively. k_1 (1/min) is the rate constant of pseudo-first-order adsorption and q_e is the adsorption capacity at equilibrium.

The pseudo-second-order kinetic model can be expressed as follows (Ho and McKay, 1999)

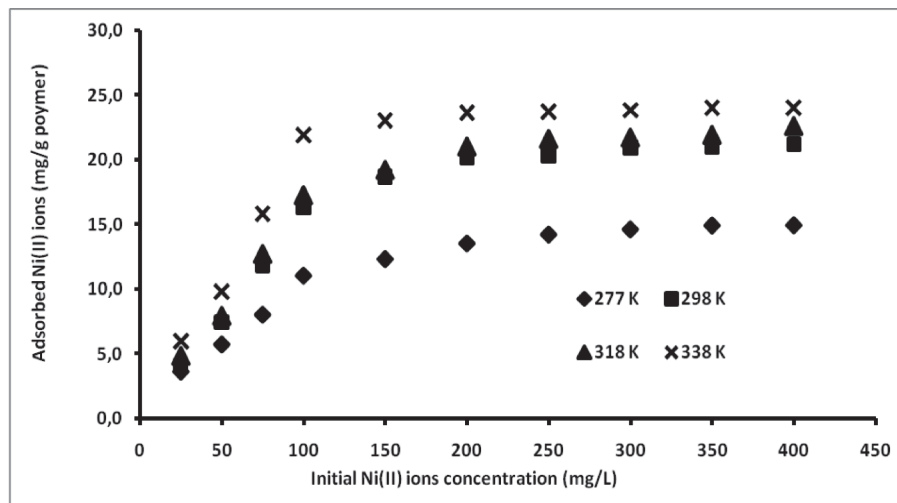


Figure 5. Effect of initial concentration of Ni(II) ions onto the m-poly(DVB-VIM) microbeads at various temperatures.

$$\frac{t}{q_t} = \frac{1}{k_2 q_e^2} + \frac{1}{q_e} t \quad (6)$$

where q_e and q_t (mg/g) have the same definitions as in Equation (5), and k_2 is the pseudo-second-order rate constant at the equilibrium ((g/mg)/min). The initial adsorbent rate h ((mg/g)/min) can be determined from k_2 and q_e values using the following equation:

$$h = k_2 q_e^2 \quad (7)$$

The modified Ritchie's-second-order kinetic model (Ritchie, 1977)

$$\frac{1}{q_t} = \frac{1}{k_R q_e t} + \frac{1}{q_e} \quad (8)$$

where q_t and q_e (mg/g) have the same definitions as in Equation (5), and k_R is the rate constant (1/min) of the modified Ritchie's-second-order kinetic model.

The intraparticle diffusion model can be described as follows (Osman et al, 2011)

$$q_t = k_i t^{1/2} \quad (9)$$

where q_t (mg/g) has the same definitions as in Equation (5), and k_i is the intraparticle diffusion rate constant ((mg/g)/min^{1/2}).

The validity of the order of the adsorption process is based on two criteria; the first one is the regression coefficients and the second one is predicted q_e values (Daoud et al, 2010). The validities of these four kinetic models for all temperatures are checked and depicted in Figure 6a-d. Among these figures, Figure 6b shows a good agreement with the pseudo-second-order kinetic model. The values of the parameters and correlation coefficient obtained from these four kinetic models are listed in Table 1. As shown in Table 1, the values of R^2 for the pseudo-second-order kinetic model are extremely high, all greater than 0.9919, followed by those of the modified Ritchie's-second-order kinetic model (Figure 6c), the pseudo-first-order kinetic model (Figure 6a) and the intraparticle diffusion model (Figure 6d), respectively. Meanwhile, the calculated q_e values obtained from the pseudo-second-order plots are found to agree with the experimental q_e values. The calculated q_e values estimated from the Ritchie's-second-order kinetic model agree slightly with the experimental q_e values. Then, because of mass transfer effects, the intraparticle diffusion models were obtained for all temperatures.

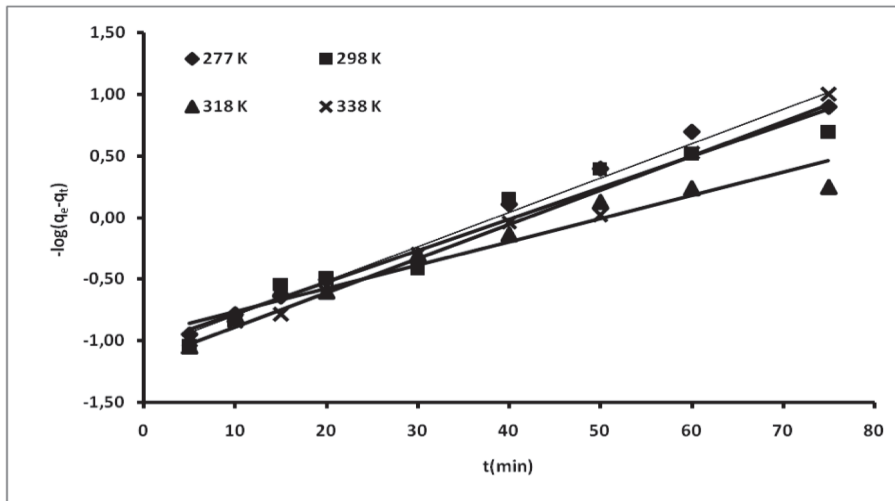


Figure 6. (a)

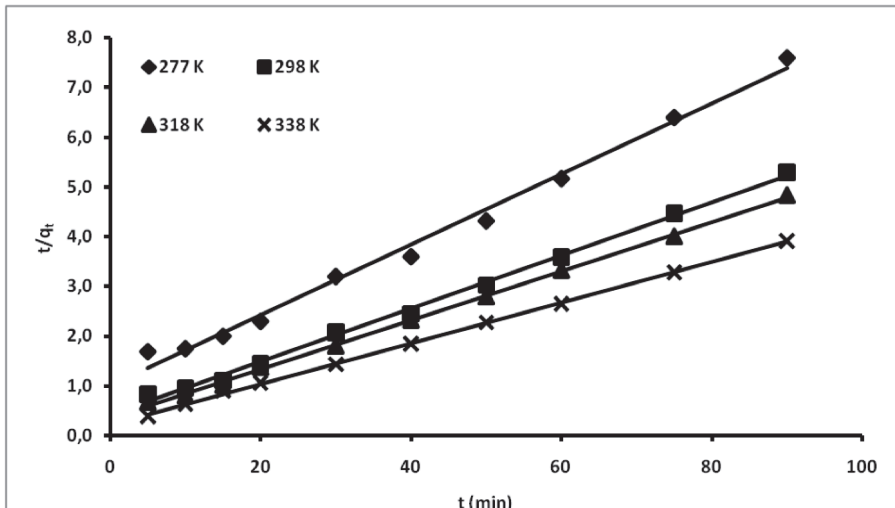


Figure 6. (b)

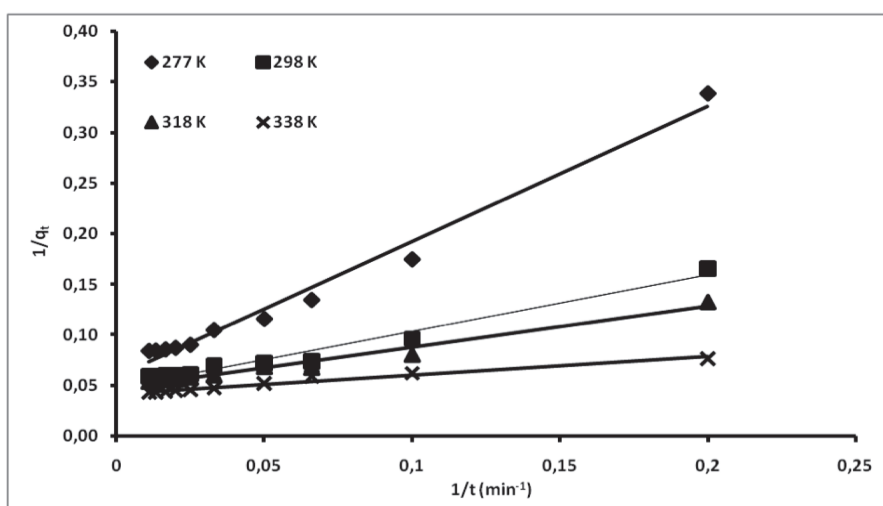


Figure 6. (c)

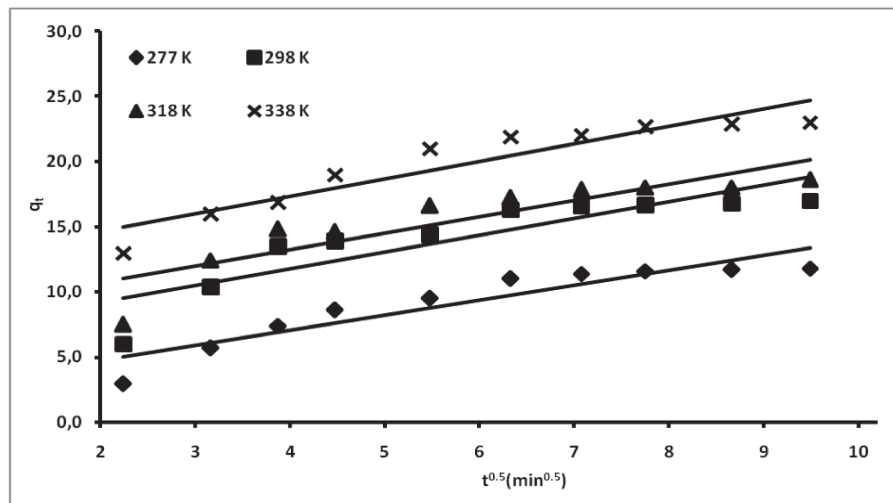


Figure 6. (d)

Figure 6. Adsorption kinetics of adsorption of Ni(II) ions by the m-poly(DVB-VIM) microbeads at different temperatures: (a) pseudo-first-order (b) pseudo-second-order (c) Ritchie's-second-order (d) intraparticle diffusion.

The plots for the intraparticle diffusion model are demonstrated in Figure 6d. The intraparticle diffusion of Ni(II) ions within the particles of the m-poly(DVB-VIM) microbeads used as an adsorbent was found to be rate-controlling in the adsorbent process. Consequently, the adsorption process could be best described by the pseudo-second-order kinetic model (Plazinski et al, 2009, Zhao et al, 2010).

The values of the pseudo-second-order rate constant, k_2 , were found to increase from 5.019×10^{-3} to 7.695×10^{-3} g/mg min, for an increase in the solution temperature of 277 to 338 K. There is a linear relationship between the k_2 and temperature (Figure 7). The adsorption rate constant is usually expressed as a function of solution temperature by the following Arrhenius type relationship (Duan et al, 2008):

$$\ln k_2 = \ln k_o - \frac{E_a}{RT} \quad (10)$$

where k_2 is the rate constant of the pseudo-second-order model of adsorption (g/(mg min)), k_o is the independent temperature factor (g/(mg min)), R is the gas constant ($8.314 \text{ J mol}^{-1} \text{ K}^{-1}$), and T is the solution temperature (K).

Therefore, the relationship between k_2 and T can be represented in an Arrhenius form as:

$$\ln k_2 = 7.9972 - \frac{621.91}{T} \quad (11)$$

From this equation, the activation energy for adsorption, E_a , is $5.171 \text{ kJ mol}^{-1}$. The magnitude of activation energy explains the type of adsorption. Two main types of adsorption can occur, physical or chemical. In physical adsorption, the equilibrium is usually attained rapidly and is easily reversible, because the energy requirements are small. The activation energy for physical adsorption is usually not more than $4.184 \text{ kJ mol}^{-1}$ ($1.0 \text{ kcal mol}^{-1}$), because the forces involved in physical adsorption are weak. Chemical adsorption is specific and involves forces much stronger than physical adsorption. Two kinds of chemical adsorption are encountered: activated and, less frequently, nonactivated. Activated chemical adsorption means that the rate varies with temperature according to a finite activation energy in the Arrhenius equation (high E_a). However, in some systems chemical adsorption occurs very rapidly, suggesting the activation energy is near zero. This is termed non-activated chemical adsorption. It is difficult to decide which mechanism is effective in the adsorption of Ni(II) ions on m-poly(DVB-VIM) microbeads, only taking activation energies into consideration. As the observed value of the acti-

vation energy of adsorption of Ni(II) ions on m-poly(DVB-VIM) microbeads is greater for less than 4.184, the adsorption process may involve both physical and chemical adsorption. (Restani et al, 2010, Fu et al, 2007).

3.7 Adsorption Isotherms

The relationship between the amount of Ni(II) ions adsorbed onto the adsorbent surface and the remaining Ni(II) ions concentration in the aqueous phase at equilibrium can be observed by the adsorption equilibrium isotherm analysis, as shown in investigating the effect of the initial concentration of Ni(II) ions. This relationship showed that the adsorption capacity increased with the equilibrium concentration of the Ni(II) ions in solution, progressively reaching saturation of the adsorbent. Adsorption isotherm curves indicate that the adsorption phenomenon may be represented by isotherms of type I, which represent a monolayer adsorption until the saturation of active sites. The adsorption isotherms were investigated using three equilibrium models, the Langmuir, Freundlich, and Dubinin-Radushkevich (D-R) isotherm models.

The Freundlich adsorption isotherm equation is given as (Freundlich, 1906),

$$q_e = K_f C_e^{1/n} \quad (12)$$

In logarithmic form,

$$\ln q_e = K_f + \frac{1}{n} \ln C_e \quad (\text{linear form}) \quad (13)$$

where q_e is the amount of metal ions adsorbed at equilibrium time (mg/g), C_e is the equilibrium concentration of the metal ions in solution (mg/L), and K_f (mg/g)(L/mg)^{1/n} and n are isotherm constants that indicate capacity and intensity of the adsorption, respectively.

The Freundlich and D-R isotherms are not as adequate as the Langmuir model ($0.9905 \leq R^2 \leq 0.9951$). The values of K_f and n were calculated from the slope and intercept of the plot $\ln q_e$ versus $\ln C_e$ (not shown). The

values of K_f and n obtained are shown in Table 2. The value of n ranges between 2.086 and 2.608. If the value of n is in the range $1 < n < 10$, the adsorption is favorable (Kara, 2009).

The Langmuir isotherm is expressed as (Langmuir, 1916)

$$\frac{C_e}{q_e} = \frac{1}{Q_L K_L} + \frac{C_e}{Q_{L_e}} \quad (14)$$

where Q_L (mg/g) is the maximum amount of Ni(II) per unit weight of the m-poly(DVB-VIM) microbeads needed to form complete monolayer coverage on the surface bound at high equilibrium Ni(II) concentration C_e , and K_L is the Langmuir constant related to the affinity of binding sites (L/mg). Q_L represents a particle limiting adsorption capacity when the surface is fully covered with Ni(II) and assists in the comparison of adsorption performance. Q_L and K_L are calculated from the slopes and intercepts of the straight lines of plot of $\frac{C_e}{q_e}$ versus C_e (not shown).

Parameters of the Langmuir and Freundlich isotherms computed are given in Table 2. The Langmuir isotherm fits quite well with the experimental data correlation coefficient ($R^2 > 0.9905$), whereas the low correlation coefficients of the Freundlich isotherm ($R^2 > 0.8206$) show poor agreement with the experimental data. Calculated maximum capacities are close to maximum capacities obtained at equilibrium Table 2. The fact that the Langmuir isotherm fits the experimental data very well may be due to homogenous distribution of active sites on the m-poly(DVB-VIM) microbeads surface, since the Langmuir equation assumes that the surface is homogeneous (Dogan et al, 2000).

Furthermore, the essential characteristic of the Langmuir isotherm can be expressed by a dimensionless separation factor called the equilibrium parameter R_L (Namasivayam and Kavita, 2002).

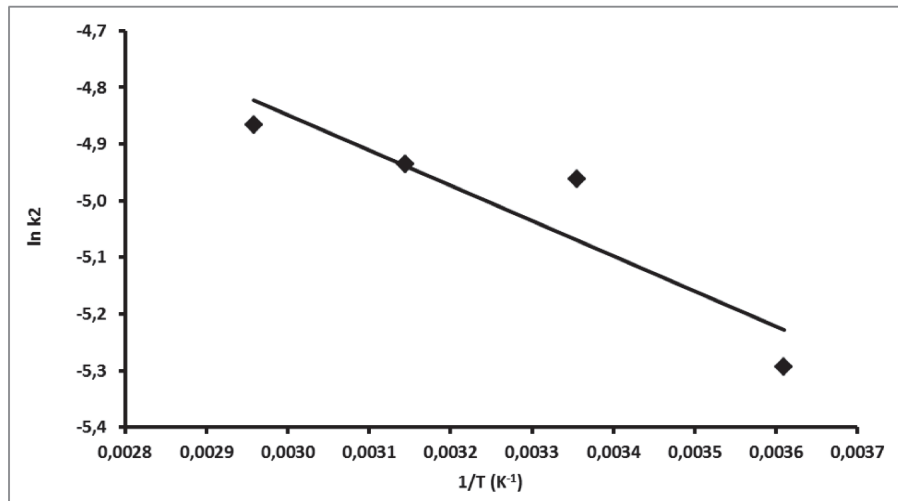


Figure 7. Arrhenius plot.

$$R_L = \frac{1}{1+KC_e} \quad (15)$$

where K is the Langmuir constant ($dm^3 mg^{-1}$) and C_e is the initial metal ion concentration ($mg dm^{-3}$).

The parameter R_L indicates the shape of the isotherm as follows:

Value of R_L Type of isotherm

$R_L > 1$	Unfavorable
$R_L = 1$	Linear
$0 < R_L < 1$	Favorable
$R_L = 0$	Irreversible

Here, the values of R_L between 0 and 1 indicate a favorable adsorption. R_L obtained are listed in Table 2. The fact that all the R_L values for the adsorption of Ni(II) ions onto the m-poly(DVB-VIM) microbeads are in the ranges 0.0854-0.7641 shows that the adsorption process was favorable.

Although the Langmuir and Freundlich isotherm models are widely used, they do not give information on the adsorption mechanism. To this aim, the equilibrium data were tested with the Dubinin-Radushkevich isotherm model (D-R

isotherm). This isotherm model predicts the nature of the adsorbate sorption onto the adsorbent and is used to calculate the mean free energy of adsorption. The nonlinear D-R isotherm is expressed as:

$$Q_e = Q_{D-R} \exp(-K_{D-R} \varepsilon^2) \quad (16)$$

and the linearized form of the equation is given as:

$$\ln Q_e = \ln Q_{D-R} - (K_{D-R} \varepsilon^2) \quad (17)$$

where Q_e is the amount of solute adsorbed per mass of adsorbent (mg/g), Q_{D-R} is the maximum adsorption capacity (mg/g), K_{D-R} is the D-R constant (mol^2/J^2), and ε is the Polanyi potential (J/mol), which can be calculated as:

$$\varepsilon = RT (\ln 1 + 1/C_e) \quad (18)$$

where R is the gas constant (J/mol K), T the absolute temperature (K), and C_e the equilibrium concentration of the adsorbate in aqueous solution (mg/L) (Laus et al, 2010, Chen et al, 2008, Tripathy and Raichur, 2008). The values of Q_{D-R} and K_{D-R} were calculated and are shown in Table 2. The mean free energy of adsorption (E_{fe}) was calculated from the K_{D-R} values using the equation:

$$E_{fe} = 1/\sqrt{-2K_{D-R}} \quad (19)$$

Table 1. Kinetic parameters for the adsorption of Ni(II) ions onto the m-poly(DVB-VIM) microbeads.

Parameters	Temperature (K)	Pseudo-first-order kinetic model			Pseudo-second-order kinetic model			Ritchie's-second order kinetic			Intraparticle diffusion model R^2
		$k_1 \times 10^2$ (L/min)	q_{eq} (mg/g)	R^2	$k_2 \times 10^3$ ((g/mg)/min)	q_{eq} (mg/g)	R^2	$k_R \times 10^2$ (L/min)	q_{eq} (mg/g)	R^2	
277	11.02	6.402	11.75	0.9862	0.998	5.019	14.10	0.9919	4.458	16.86	0.9834 1.155
298	16.35	5.850	10.76	0.9553	2.448	7.007	18.69	0.9972	8.641	20.83	0.9706 1.286
318	17.24	4.330	9.968	0.9303	2.945	7.186	20.24	0.9989	11.65	21.19	0.9748 1.259
338	23.07	6.356	14.51	0.9849	4.600	7.695	23.45	0.9994	22.95	23.64	0.9654 1.343
											0.8733

Table 2. Parameters of Langmuir, Freundlich and Dubinin-Raduskevich isotherm models, for the adsorption of Ni(II) ions onto the m-poly(DVB-VIM) microbeads.

Parameters Temperature (K)	Langmuir isotherm constants			Freundlich isotherm constants			Dubinin-Raduskevich isotherm constants			R^2	
	$K_L \times 10^2$ (L/mg)	Q_L (mg/g)	R^2	R_L range	K_F (mg/g)(L/mg) $^{1/n}$	n	R^2	Q_{D-R} (mg/g)	$K_{D-R} \times 10^9$ (mol $^{2}/J^2$)	E_{fe} (kJ/mol)	
277	1.235	18.59	0.9906	0.1684 - 0.7641	1.016	2.086	0.9135	45.75	-7.322	8.264	0.9486
298	1.816	24.75	0.9930	0.1210 - 0.6878	2.009	2.363	0.9004	56.73	-5.455	9.574	0.9342
318	1.875	25.91	0.9951	0.1176 - 0.6808	2.243	2.425	0.9139	57.55	-4.626	10.40	0.9435
338	2.677	27.03	0.9905	0.0854 - 0.5991	2.974	2.668	0.8206	61.25	-3.835	11.42	0.8662

The E_{fe} value is used to ascertain the type of adsorption process under consideration. If this value is between 8 and 16 kJ mol⁻¹, the adsorption process can be assumed to involve chemical adsorption. On the other hand, values lower than 8 kJ mol⁻¹ indicate that the adsorption process is of a physical ion exchange mechanism (Ozcan et al, 2005, Unlu and Ersoz, 2006, Tassist et al, 2010). In this study, the D-R isotherm model is in the ranges 0.8662-0.9486 and the E_{fe} values obtained using the D-R constant, in the non-linear form, were 8.264 kJ mol⁻¹ for 277 K, 9.574 kJ mol⁻¹ for 298 K, 10.40 kJ mol⁻¹ for 318 K, and 11.42 kJ mol⁻¹ for 338 K, indicating that the adsorption of Ni(II) ions onto the m-poly(DVB-VIM) occurs via a chemical ion exchange mechanism process for all the temperatures.

3.8 Adsorption Thermodynamics

Temperature dependence of the equilibrium constant, K_L , can be used to determine the thermodynamic parameters (Zhou et al, 2009). The van't Hoff equation is used to evaluate the variation of the equilibrium constant with temperature. The integrated form of this equation is given as:

$$\ln K_L = \frac{\Delta S^\circ}{R} - \frac{\Delta H^\circ}{R} \left(\frac{1}{T}\right) \quad (20)$$

The enthalpy (ΔH°) and entropy (ΔS°) changes of the process can be determined from the slope and intercept of the line obtained by plotting $\ln K_L$ versus $1/T$. The equation of free energy for each temperature is then obtained as:

$$\Delta G^\circ = \Delta H^\circ - T\Delta S^\circ \quad (21)$$

From Equation (21), the Gibbs free energy change of adsorption (ΔG°) was calculated as -15.17, -17.27, -18.52 and -20.68 kJ/mol for the adsorption of Ni(II) ions onto the m-poly(DVB-VIM) microbeads at 277, 298, 318, and 338 K, respectively. The negative ΔG° values indicated that the adsorption of Ni(II) ions onto the m-poly(DVB-VIM) microbeads was thermodynamically feasible and spontaneous. The enthal-

py (ΔH°) and entropy (ΔS°) changes were determined as 9.032 kJ/mol and 87.54 J/mol K, respectively, from $\ln K_L$ versus $1/T$ plot (Figure 8). The positive value of ΔH° confirmed the endothermic character of the adsorption process. The positive values of ΔS° also revealed the increase of randomness at the solid-solute interface during the adsorption of Ni(II) ions onto the m-poly(DVB-VIM) microbeads. The low value of ΔS° indicated that no remarkable changes on entropy occur.

3.9 Desorption and Repeated Use

The use of an adsorbent in the adsorption process depends not only on the adsorption capacity, but also on how well the adsorbent can be regenerated and used again. For repeated use of an adsorbent, adsorbed metal ions should be easily desorbed under suitable conditions. Desorption of the adsorbed Ni(II) ions from the m-poly(DVB-VIM) microbeads was also studied in a batch experimental system. Desorption experiments resulted in desorption of Ni(II) ions after 1 h of contact with HNO₃ solutions (0.1 mol/L, desorption percentage 99%). Repeated use of HNO₃ solutions of the m-poly(DVB-VIM) microbeads showed that the adsorption-desorption process is a reversible process. Ten cycles of adsorption-desorption experiments were conducted to examine the capability of the m-poly(DVB-VIM) microbeads to retain Ni(II) ions removal capacity. The adsorption capacity of the mesoporous m-poly(DVB-VIM) microbeads decreased only 3% during the 10 adsorption-desorption cycles.

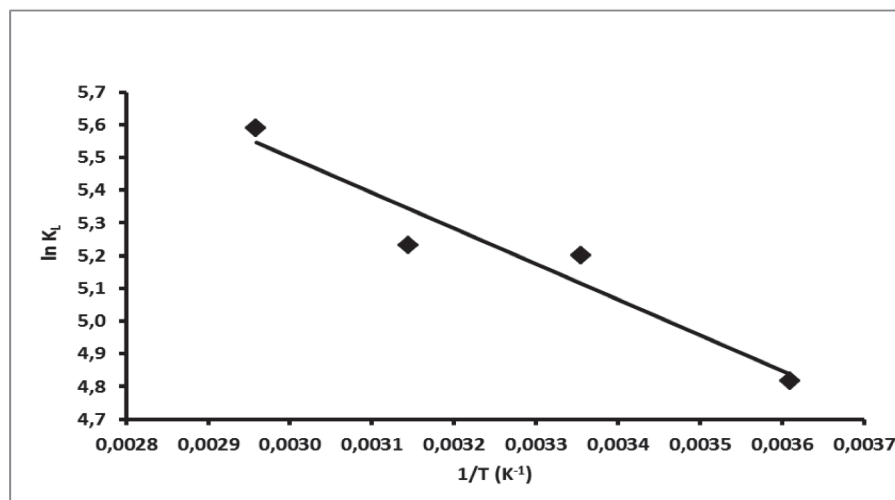


Figure 8. The plot of $\ln K_L$ versus $1/T$ for the determination of thermodynamic parameters for adsorption of Ni(II) ions onto the m-poly(DVB-VIM) microbeads.

4. CONCLUSIONS

In this study, the magnetic-poly(divinylbenzene-co-vinylimidazole) (m-poly(DVB-VIM)) microbeads (average diameter = 53–212 μm) were synthesized and characterized. The physicochemical parameters affecting adsorption of Ni(II) ions from aqueous solutions were investigated. The pseudo-first-order kinetic model, pseudo-second-order kinetic model, modified Ritchie's-second-order kinetic model, and intraparticle diffusion model were used for testing dynamic experimental data at the initial concentration. The adsorption process could be best described by the pseudo-second-order kinetic model. The equilibrium data were analyzed using the Langmuir, Freundlich, and Dubinin-Radushkevich isotherm models. It was found that the adsorption of Ni(II) ions was well fitted to the Langmuir equation. Thermodynamic parameters revealed that the adsorption was thermodynamically feasible, spontaneous, and endothermic in nature. Most importantly, the m-poly(DVB-VIM) microbeads exhibited a high stability and good reusability. This showed that the m-poly(DVB-VIM)] microbeads in this study have a great potential in practical application.

ACKNOWLEDGMENT

This work was supported by the Research Foundation of Uludag University (Project No: UAP(F)-2011/35).

REFERENCES

- Akgol, S., Kusvuran, E., Kara, A., Senel, S. and Denizli, A. (2006). Porous dye affinity beads for nickel adsorption from aqueous solutions: A kinetic study. *Journal Applied Polymer Science* 100(6), 5056-5065.
- Bajpai, S.K. and Johnson, S. (2007). Removal of Ni^{2+} ions from aqueous solution by sorption into poly(acrylamide-co-sodium acrylate) hydrogels. *Journal of Macromolecular Science A: Pure and Applied Chemistry* 44(3), 285-290.
- Bayramoglu, G., Senel, A.U. and Arica, M.Y. (2006). Effect of spacer-arm and Cu(II) ions on performance of l-histidine immobilized on poly(GMA/MMA) beads as an affinity ligand for separation and purification of IgG. *Separation and Purification Technology* 50(2), 229-239.
- Chen, A.H., Liu, S.C. and Chen, C.Y. (2008). Comparative adsorption of Cu(II), Zn(II) and Pb(II) ions in aqueous solution on the

- crosslinked chitosan with epichlorohydrin. *Journal of Hazardous Materials* 154(1-3), 184-191.
- Daoud, F.B., Kaddour, S. and Sadoun, T. (2010). Adsorption of cellulase *Aspergillus niger* on a commercial activated carbon: Kinetics and equilibrium studies. *Colloids Surface B*: 75(1), 93-99.
- Dogan, M., Alkan, M. And Onganer, Y. (2000). Adsorption of methylene blue on perlite from aqueous solutions. *Water Air Soil Pollution* 120(3-4), 229-248.
- Duan, G., Zhang, C., Li, A., Yang, X., Lu, L. and Wang, X. (2008). Preparation and characterization of mesoporous zirconia made by using a poly (methyl methacrylate) template. *Nanoscale Research Letter* 3(3), 118-122.
- Freundlich, H.M.F. (1906). Über die adsorption in lösungen, *Zeitschrift für Physikalische Chemie (Leipzig)*, 57A, 385-470.
- Fu, L.J., Zhang, T., Cao, Q., Zhang, H.P. and Wu, Y.P. (2007). Preparation and characterization of three-dimensionally ordered mesoporous titania microparticles as anode material for lithium ion battery. *Electrochemistry Communications* 9(8), 2140-2144.
- Ghassabzadeh, H., Mohadespour, A., T-Mostaedi, M., Zaheri, P., Maragheh, M.G. and Taheri, H. (2010). Adsorption of Ag, Cu and Hg from aqueous solutions using expanded perlite. *Journal of Hazardous Materials* 177(1-3), 950-955.
- Hanafiah, M.A.K.M., Zakaria, H. and Ngah, W.S.W. (2010). Base treated cogon grass (*Imperata cylindrica*) as an adsorbent for the removal of Ni(II): Kinetic, isothermal and fixed-bed column studies. *Clean – Soil, Air, Water* 38(3), 248-256.
- Hanafiah, M.A.K.M., Zakaria, H. and Wan Ngah, W.S. (2009). Preparation, characterization, and adsorption behavior of Cu(II) ions onto alkali-treated weed (*Imperata cylindrica*) leaf powder. *Water Air Soil Pollution* 201(1-4), 43-53.
- Ho, Y.S. and McKay, G. (1999). Pseudo-second order model for sorption processes. *Process Biochem.* 34(5), 451-465.
- Hua, M., Zhang, S., Pan, B., Zhang, W. and Zhang, L. Lv, Q. (2011). Heavy metal removal from water/wastewater by nanosized metal oxides: A review. *Journal of Hazardous Materials* 211-212, 317-331.
- Kara, A. (2009). Adsorption of Cr(VI) ions onto poly(ethylene glycol dimethacrylate-1-vinil-1,2,4-triazol). *Journal Applied Polymer Science* 114(2), 948-955.
- Kara, A., Uzun, L., Besirli, N. and Denizli, A. (2004). Poly(ethylene glycol dimethacrylate-n-vinyl imidazole) beads for heavy metal removal. *Journal of Hazardous Materials* 106(2-3), 93-99.
- Lagergren, S. (1898). Zur theorie der sogenannten adsorption gelöster stoffe. *Kungliga Svenska Vetenskapsakademiens. Handlingar* 24(4), 1-39.
- Langmuir, I. (1916). The constitution and fundamental properties of solids and liquids. *Journal of the American Chemistry Society* 38, 2221-2295.
- Laus, R., Costa, T.G., Szpoganicz, B. and Fávere, V.T. (2010). Adsorption and desorption of Cu(II), Cd(II) and Pb(II) ions using chitosan crosslinked with epichlorohydrin-triphosphate as the adsorbent. *Journal of Hazardous Materials* 183(1-3), 233-241.
- Mahdavian, A.R. and Mirrahim, M.A.S. (2010). Efficient separation of heavy metal cations by anchoring polyacrylic acid on superparamagnetic magnetite nanoparticles through surface modification. *Chemical Engineering Journal* 159(1-3), 264-271.
- Monier, M., Ayad, D.M., Wei, Y. and Sarhan, A.A. (2010). Adsorption of Cu(II), Co(II), and Ni(II) ions by modified magnetic chi-

- tosan chelating resin. *Journal of Hazardous Materials* 177(1-3), 962-970.
- Namasivayam, C. and Kavita, D. (2002). Removal of congo red from water by adsorption on to activated carbon prepared from coir pith, an agricultural solid waste. *Dyes Pigment* 54(1), 47-58.
- Ngah, W.S.W. and Fatinathan, S. (2010). Adsorption characterization of Pb(II) and Cu(II) ions onto chitosan-tripolyphosphate beads: Kinetic, equilibrium and thermodynamic studies. *Journal of Environmental Management* 91(4), 958-969.
- Olgun, A. and Atar, N. (2011). Removal of copper and cobalt from aqueous solution onto waste containing boron impurity. *Chemical Engineering Journal* 167(1), 140-147.
- Osman, B., Kara, A. and Besirli, N. (2011). Immobilization of glucoamylase onto Lewis metal ion chelated magnetic affinity sorbent: kinetic, isotherm and thermodynamic studies. *Journal of Macromolecular Science Pure & Applied Chemistry* 48(5), 387-399.
- Ozay, O., Ekici, S., Baran, Y., Aktas, N. and Sahiner, N. (2009). Removal of toxic metal ions with magnetic hydrogels. *Water Research* 43(17), 4403-4411.
- Ozcan, A., Ozcan, A.S., Tunali, S., Akar, T. and Kiran, I. (2005). Determination of the equilibrium, kinetic and thermodynamic parameters of adsorption of copper(II) ions onto seeds of capsicum annum. *Journal of Hazardous Materials* 124(1-3), 200-208.
- Ozer, A., Ozer, D. and Ozer, A. (2004). The adsorption of copper(II) ions on to dehydrated wheat bran (DWB): Determination of the equilibrium and thermodynamic parameters. *Process Biochemistry* 39(12), 2183-2191.
- Patil, A.K. and Shrivastava, V.S. (2010). Adsorption of Ni(II) from aqueous solution on *Delonix regia* (*Gulmohar*) tree bark. *Ar. Applied Science Resource* 2(2), 404-413.
- Plazinski, W., Rudzinski, W. and Plazinska, A. (2009). Theoretical models of sorption kinetics including a surface reaction mechanism: A review. *Adv. Colloid Interface Science* 152(1-2), 2-13.
- Restani, R.B., Correia, V.G., Bonifácio, V.D.B. and A.-Ricardo, A. (2010). Development of functional mesoporous microparticles for controlled drug delivery. *Journal of Supercrit. Fluids* 55(1), 333-339.
- Ritchie, A.G. (1977). Alternative to the Elovich equation for the kinetics of adsorption of gases on solids. *Journal of Chemistry Soc. Faraday Trans.* 73, 1650-1653.
- Senel, S., Uzun, L., Kara, A. and Denizli, A. (2008). Heavy metal removal from synthetic solutions with magnetic beads under magnetic field. *Journal of Macromolecular Science Pure & Applied Chemistry A* 45(8), 635-642.
- Souza, K.C., Ardisson, J.D. and Sousa, E.M.B. (2009). Study of mesoporous silica/magnetite systems in drug controlled release. *Journal of Materials Science: Materials in Medicine* 20(2), 507-512.
- Strkalj, A., Radenovic, A. and Malina, J. (2010). Nickel adsorption onto carbon anode dust modified by acetic acid and KOH. *Journal of Mining and Metallurg Section B-Metall.* 46 (1), 33-40.
- Taqvi, S.I.H., Hasany, S.M. and Bhanger, M.I. (2008). Sorptive potential of beach sand to remove Ni(II) ions: An Equilibrium isotherm study. *Clean – Soil, Air, Water* 36(4), 366-372.
- Tassist, A., Lounici, H., Abdi, N. and Mameri, N. (2010). Equilibrium, kinetic and thermodynamic studies on aluminum biosorption by a mycelial biomass (*Streptomyces rimosus*). *Journal of Hazardous Materials* 183(1-3), 35-43.

- Tripathy, S.S. and Raichur, A.M. (2008). Abatement of fluoride from water using manganese dioxide-coated activated alumina. *Journal Hazardous Materials* 153(3), 1043-1051.
- Tseng, J.Y., Chang, C.Y., Chen, Y.H., Chang, C.F. and Chiang, P.C. (2007). Synthesis of micro-size magnetic polymer adsorbent and its application for the removal of Cu(II) ion. *Colloids Surface A*: 295(1-3), 209-216.
- Unlu, N. and Ersoz, M. (2006). Adsorption characteristics of heavy metal ions onto a low cost biopolymeric sorbent from aqueous solutions. *Journal Hazardous Materials B* 136(2), 272-280.
- Wang, X.S., Ren, J.J., Lu, H.J., Zhu, L., Liu, F., Zhang, Q. and Xie, J. (2010). Removal of Ni(II) from aqueous solutions by nanoscale magnetite. *Clean–Soil Air Water* 38(12), 1131-1136.
- Zhao, Z., Wang, X., Zhao, C., Zhu, X. and Du, S. (2010). Adsorption and desorption of antimony acetate on sodium montmorillonite. *Journal of Colloid Interface Science* 345(2), 154-159.
- Zhou, Y.T., White, C.B., Nie, H.L. and Zhu, L.M. (2009). Adsorption mechanism of Cu²⁺ from aqueous solution by chitosan-coated magnetic nanoparticles modified with α -ketoglutaric acid. *Colloids Surface B: Biointerfaces* 74(1), 244-252.

